Parameterization of Subgrid Scale Barotropic and Baroclinic Eddies in Quasi-geostrophic Models: Anticipated Potential Vorticity Method

ROBERT SADOURNY AND CLAUDE BASDEVANT

Laboratoire de Météorologie Dynamique, Ecole Normale Supérieure, 24 rue Lhomond, 75231 Paris Cedex 05, France

(Manuscript received 12 September 1984, in final form 25 February 1985)

ABSTRACT

A lateral diffusion scheme designed to efficiently parameterize the subgrid scale fluxes associated with barotropic and baroclinic transients is presented and tested on a quasi-geostrophic, two layer model, with large-scale thermal forcing. The scheme is based on formal energy conservation and potential enstrophy dissipation. At very coarse resolutions, where the cutoff scale is of the order of the internal radius of deformation, the diffusion scheme is shown to produce a realistic amount of potential-to-kinetic energy conversions, and realistic amplitudes of the large-scale barotropic modes.

1. Introduction

One of the current trends of climate modeling is an increasing need for very long-term simulations spanning decades to centuries or more addressing the problems of climate variability or tendency, and a need for larger statistical ensemble simulations, to increase statistical significance of signal-to-noise ratios. In view of the computational burden involved by extending the integration range or multiplying the number of simulations, there is a need for more efficient, economical, low-resolution models on which repeated long simulations could be carried out at low computational cost without too much quality loss. This shift towards lower resolution models has already begun in the last decade; it has been facilitated by the development of spectral techniques. In the present state of the art, however, it seems difficult to reduce resolution beyond, say, "triangular 20" in spherical harmonics, without severely damaging the representation of baroclinic instability processes. Our progress in low-resolution climate modeling will therefore be subordinate to at least some degree of success in parameterizing baroclinic instability. We are speaking here of atmosphere models; but the problem appears even more critical when looking at ocean models, for which simultaneous explicit treatment of baroclinic eddies and basin scale gyres remains beyond present computing capabilities.

The question of how to parameterize eddy heat fluxes has already been raised by a number of authors, but always from the standpoint of the linear theory (Saltzman, 1968; Green, 1970; Stone, 1974; Held, 1978; Stone, 1978) which considers the growth of a single wave superimposed on a parallel quasi-geostrophic flow with vertical shear. Here we shall address the problem from the more general standpoint of parameterizing subgrid scale eddy fluxes within the framework of fully developed quasi-geostrophic turbulence theory. It has been shown by Hoyer and Sadourny (1982) that the driving mechanism for baroclinic instability could be understood as the need of quasi-geostrophic flow to dissipate its potential enstrophy while conserving its total energy. The trapping of energy within scales larger than the internal radius of deformation, associated to a cascade of potential enstrophy towards smaller scales, means a necessary conversion of potential energy into kinetic energy in the vicinity of the internal radius of deformation. It was then shown by Sadourny and Hoyer (1982) that ordinary diffusion schemes, being energy dissipating, inhibit significantly the baroclinic instability processes as soon as the cutoff scale becomes of the order of the radius of deformation. In the meantime, a new type of lateral diffusion scheme was developed (Sadourny and Basdevant, 1981), which was based on the two main driving mechanisms of quasi-geostrophic turbulence: energy conservation, potential enstrophy dissipation. This scheme was successfully tried first on barotropic flows (Basdevant and Sadourny, 1983), but in view of what we just said, it looked even more promising as a baroclinic instability parameterization scheme. Therefore this scheme, renamed the "Anticipated Potential Vorticity Method" was later applied to a quasi-geostrophic two-layer model; we discuss here its performance regarding the parameterization of baroclinic instability.

2. The Anticipated Potential Vorticity Method (APVM)

The Anticipated Potential Vorticity Method (APVM) was originally introduced by Sadourny and Basdevant (1981) for the barotropic vorticity equation

only. We give here a more general formulation valid for the primitive equations in the entropy coordinate.

Let s be any function of thermodynamic entropy. The equation of motion in s coordinate reads

$$\frac{\partial \mathbf{V}}{\partial t} + \eta \mathbf{N} \times r\mathbf{V} + \text{grad}\left(S + \frac{V^2}{2}\right) = 0, \quad (1)$$

where $\mathbf{V}$ is horizontal velocity, η potential vorticity

$$\eta = (f + \text{rot}\mathbf{V})/r, \quad (2)$$

f Coriolis parameter, $r = -\partial p/\partial s$ is a pseudo-density, p pressure, $\mathbf{N}$ the vertical upward unit vector and S the dry static energy or Montgomery potential (geopotential plus enthalpy). The continuity equation reads

$$\frac{\partial r}{\partial t} + \text{div}(r\mathbf{V}) = 0. \quad (3)$$

We first require that our parameterization be energy conserving. This is enforced locally by requiring lateral diffusion to act perpendicular to velocity; then the modified equation of motion reads

$$\frac{\partial \mathbf{V}}{\partial t} + (\eta - D)\mathbf{N} \times r\mathbf{V} + \text{grad}\left(S + \frac{V^2}{2}\right) = 0, \quad (4)$$

which yields a potential vorticity equation of the form

$$\frac{D\eta}{Dt} - \frac{1}{r}\text{div}(Dr\mathbf{V}) = 0; \quad (5)$$

here D is, for the moment, arbitrary, but we have to require that diffusion be potential-enstrophy dissipating. On an isentropic surface which does not cross upper or lower boundaries, potential enstrophy is defined as

$$Z(s) = \int\int_\Omega \frac{\eta^2}{2} r dx dy, \quad (6)$$

where Ω is the horizontal flow domain. From (5) and (6), we get:

$$\frac{dZ(s)}{dt} = -\int\int_\Omega D\mathbf{V} \cdot \text{grad}\eta r dx dy. \quad (7)$$

It is now easy to construct a general form of D which ensures potential enstrophy dissipation:

$$D = \theta r^{-1/2} L(r^{1/2} V \cdot \text{grad}\eta); \quad (8)$$

here θ is a time scale and L is a nondimensional, nonnegative definite linear operator. Equation (8) yields a rate of potential enstrophy dissipation

$$-\frac{dZ(s)}{dt} = \theta \int\int_\Omega (r^{1/2} V \cdot \text{grad}\eta) L (r^{1/2} V \cdot \text{grad}\eta) dx dy, \quad (9)$$

a (density weighted) quadratic form of potential vorticity advection rate. Note that dissipation here becomes inefficient as soon as the motion is stationary.[1] If we neglect density weighting, we can interpret (4, 8) by saying that the diffusion effect is obtained by choosing an upwind estimate of potential vorticity in the rotation term of the equation of motion. If $L = 1$, we have a simple upwind estimate or anticipation of potential vorticity value by a time lag θ: hence the name "Anticipated Potential Vorticity Method" (APVM).

In the general case, L has a complete set of orthonormal eigenfunctions $\Lambda_k(x, y)$, corresponding to eigenvalues $\lambda_k \geq 0$. It is natural to choose Λ_k as the eigenfunctions of the Laplacian (for example, complex exponentials on the periodic plane) and then define θL as a set of scale-dependent time lags $\{\theta_k\}$. The spectral transform of (5) then reads

$$\frac{d}{dt}\frac{1}{2}\|(r^{1/2}\eta)_k\|^2 + T_k = -\text{Re}\sum_{q=k+p}(r^{1/2}\mathbf{V})_{-p} \times \mathbf{k}\eta_{-k}\theta_q \sum_{q=l+s}(r^{1/2}\mathbf{V})_l \cdot \mathbf{s}\eta_s. \quad (10)$$

We expect that the subgrid scales have little effect on scales much larger than the cutoff scale ($k \ll k_c$). We thus choose $\theta_q \approx 0$ for $k \ll k_c$, and a cusp-like behavior near k_c, where the subgrid scale influence becomes important. Qualitatively, the time scale spectrum θ_k must be reminiscent of the forms already obtained in other parameterization schemes (Leith, 1968; Kraichnan, 1976; Basdevant, Lesieur and Sadourny, 1978); the situation, however, is made more complex here by the strong nonlinearity of the diffusion operator, which yields the double convolution term in the spectral expansion (10).

The simplest way to qualitatively meet these requirements is to choose

$$L = k_c^{-2\alpha}(-\nabla^2)^\alpha,$$

or in terms of time lags

$$\theta_k = \theta(k/k_c)^{2\alpha}.$$

The set of parameters $\{\theta_k\}$ then reduces to two parameters θ and α only; α measures the space selectivity of the diffusion scheme, while θ corresponds to the eddy-turnover time scale at $k = k_c$, which can be estimated from phenomenological arguments as proportional to the inverse of the square root of kinetic enstrophy $\tilde{Z}$.

3. Numerical modeling

The APVM has already been successfully tested on decaying and forced quasi-geostrophic barotropic tur-

[1] In particular, D vanishes for parallel ("zonal") flow, like the original nonlinear terms; diffusion becomes active as soon as the flow is slightly perturbed.

bulence simulations (Basdevant and Sadourny, 1983). Its main advantages compared to the simpler iterated Laplacian ("superviscosity") formulation

$$\frac{\partial \eta}{\partial t} + \mathbf{V} \cdot \text{grad}\eta + \nu_\beta(-\nabla^2)^\beta \eta = 0 \qquad (11)$$

is that the artificial viscosity range, concentrated in the close vicinity of the cutoff wavenumber for large values of β, disappears completely with the APVM. This was already the case with lateral diffusion based on closure assumptions (Basdevant, Lesieur and Sadourny, 1978), with the important difference that the k^{-3} slope is imposed in closure model diffusion, while the slope is free to adjust to any value dictated by nonlinear dynamics in the APVM. This is an important improvement, since some doubts concerning the validity of the classical phenomenology have recently been expressed (Basdevant, Legras, Sadourny and Béland, 1981; McWilliams, 1984; Babiano, Basdevant and Sadourny, 1984; Babiano, Basdevant, Legras and Sadourny, 1984). Here we shall concentrate on baroclinic two-layer flow, and the ability of the APVM to simulate the subgrid scale potential-to-kinetic energy conversions.

a. Basic formulation

The numerical model used here is derived from the plane-periodic pseudospectral barotropic model of Basdevant *et al.* (1981). The generic equation reads

$$\frac{\partial \eta^l}{\partial t} + J(\psi^l, \eta^l) + P^l = H^l + F^l \qquad (12)$$

where $l = 1, 2$ refers to layer index, J to the two-dimensional Jacobian, ψ to streamfunction; H, F and P refer to heating, friction and subgrid scale parameterization, respectively. Denoting by λ the internal deformation wavenumber, the Fourier coefficients $\eta_\mathbf{k}$, $\psi_\mathbf{k}$ are related by

$$\eta_\mathbf{k}^1 = -k^2\psi_\mathbf{k}^1 + \frac{\lambda^2}{2}(\psi_\mathbf{k}^2 - \psi_\mathbf{k}^1),$$

$$\eta_\mathbf{k}^2 = -k^2\psi_\mathbf{k}^2 + \frac{\lambda^2}{2}(\psi_\mathbf{k}^1 - \psi_\mathbf{k}^2).$$

Instead of layers, we may equivalently consider barotropic and baroclinic vertical modes:

$$\hat{\eta}_\mathbf{k}^0 = \frac{1}{2}(\eta_\mathbf{k}^1 + \eta_\mathbf{k}^2),$$

$$\hat{\eta}_\mathbf{k}^1 = \frac{1}{2}(\eta_\mathbf{k}^2 - \eta_\mathbf{k}^1),$$

and similarly for $\hat{\psi}_\mathbf{k}^0$, $\hat{\psi}_\mathbf{k}^1$, $\hat{H}_k^0$, $\hat{H}_\mathbf{k}^1$, etc. We have

$$\hat{\eta}_\mathbf{k}^0 = -k^2\hat{\psi}_\mathbf{k}^0,$$

$$\hat{\eta}_\mathbf{k}^1 = -(k^2 + \lambda^2)\hat{\psi}_\mathbf{k}^1.$$

b. Thermal forcing

Since H^l is a thermal forcing term, it is best defined in modal form as pure baroclinic forcing: $\hat{H}_\mathbf{k}^0 = 0$. $\hat{H}_k^1$ is defined through a baroclinic streamfunction source $\hat{\psi}_*^1(x, y)$:

$$\hat{H}_\mathbf{k}^1 = -(k^2 + \lambda^2)\hat{\psi}_{*\mathbf{k}}^1.$$

In the experiments described here, the forcing function $\hat{\psi}_*^1(x, y)$ was implicitly defined by the relation

$$\hat{\psi}_*^1[x, y + \epsilon(1 + \sin y)\sin(x - y)] = a \cos y, \qquad (13)$$

with $-\pi < x \leqslant \pi$, $-\pi < y \leqslant \pi$, $\epsilon = \pi/10$; it is shown in Fig. 1. We have maximum heating at $y = 0$, maximum cooling at $y = \pm\pi$; the thermal forcing is roughly zonal for $-\pi < y < 0$, but has a superimposed tilted wave pattern for $0 < y < \pi$, with strongest gradient around $x = \pi/2$, $y = \pi/2$. The heating amplitude a was not taken constant in time, but reevaluated at every time step to ensure a constant rate of energy input. In regime conditions, however, the fluctuations of a around its time average were observed to be small (less than 10%).

This nonzonal forcing was selected to be reminiscent of atmospheric forcing with its tilted planetary wave pattern in the Northern Hemisphere. Experiments with purely zonal forcing have also been performed, leading to qualitatively similar results; they are not described here.

c. Friction

Friction is prescribed as linear and purely barotropic:

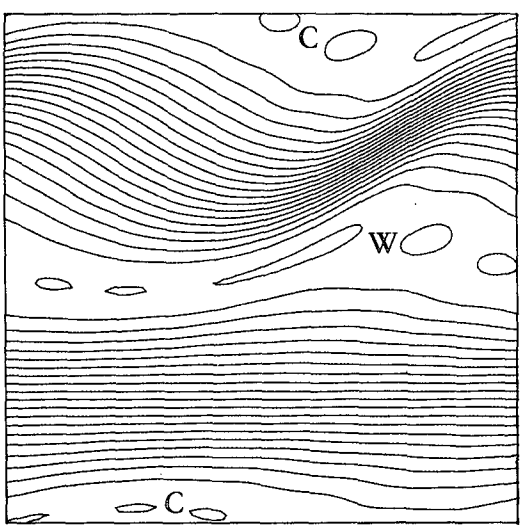

FIG. 1. Large-scale heating field used in the experiments. *W*: maximum warming area. *C*: maximum cooling area.

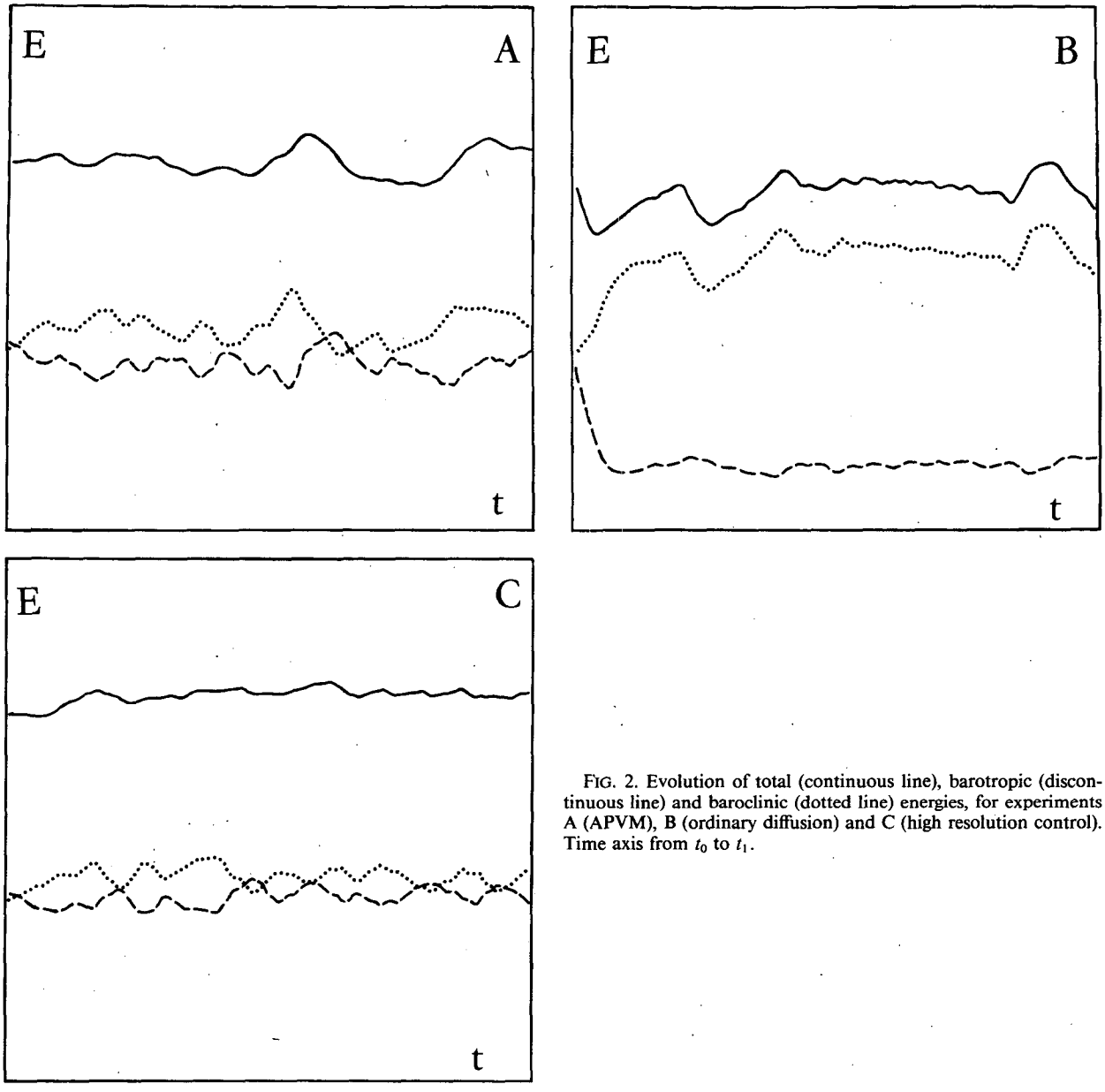

FIG. 2. Evolution of total (continuous line), barotropic (discontinuous line) and baroclinic (dotted line) energies, for experiments A (APVM), B (ordinary diffusion) and C (high resolution control). Time axis from t_0 to t_1.

$$\hat{F}_{\mathbf{k}}^{0} = \nu_F \hat{\psi}_{\mathbf{k}}^{0}, \quad \hat{F}_{\mathbf{k}}^{1} = 0. \tag{14}$$

Here we have assumed that the main effect of friction is to remove energy from the barotropic large scales where it tends to accumulate due to the reverse energy cascade.

d. Subgrid scale parameterization

Here we consider two versions. One uses the APVM formulation with an iterated Laplacian for L:

$$P^l = -\theta k_c^{-2\alpha} J\{\psi^l, (-\nabla^2)^\alpha J(\psi^l, \eta^l)\}, \tag{15}$$

and $\alpha = 8$; P^l is integrated in time using an explicit forward formulation. A heuristic stability criterion based on (15) can be written as

$$\Delta t_{\text{APVM}}\theta/\Delta t_{\text{Advection}}{}^2 \leqslant 1.$$

With $\Delta t_{\text{Advection}}$ being of the order of $\theta \sim Z^{-1/2}$, Δt_{APVM} should be of the same order. Our numerical integrations were actually stable for

$$\Delta t_{\text{APVM}} = \Delta t_{\text{Advection}}.$$

The other version uses the more classical iterated Laplacian

$$P^l = \frac{1}{\tau} k_c^{-2\beta}(-\nabla^2)^\beta \eta^l, \tag{16}$$

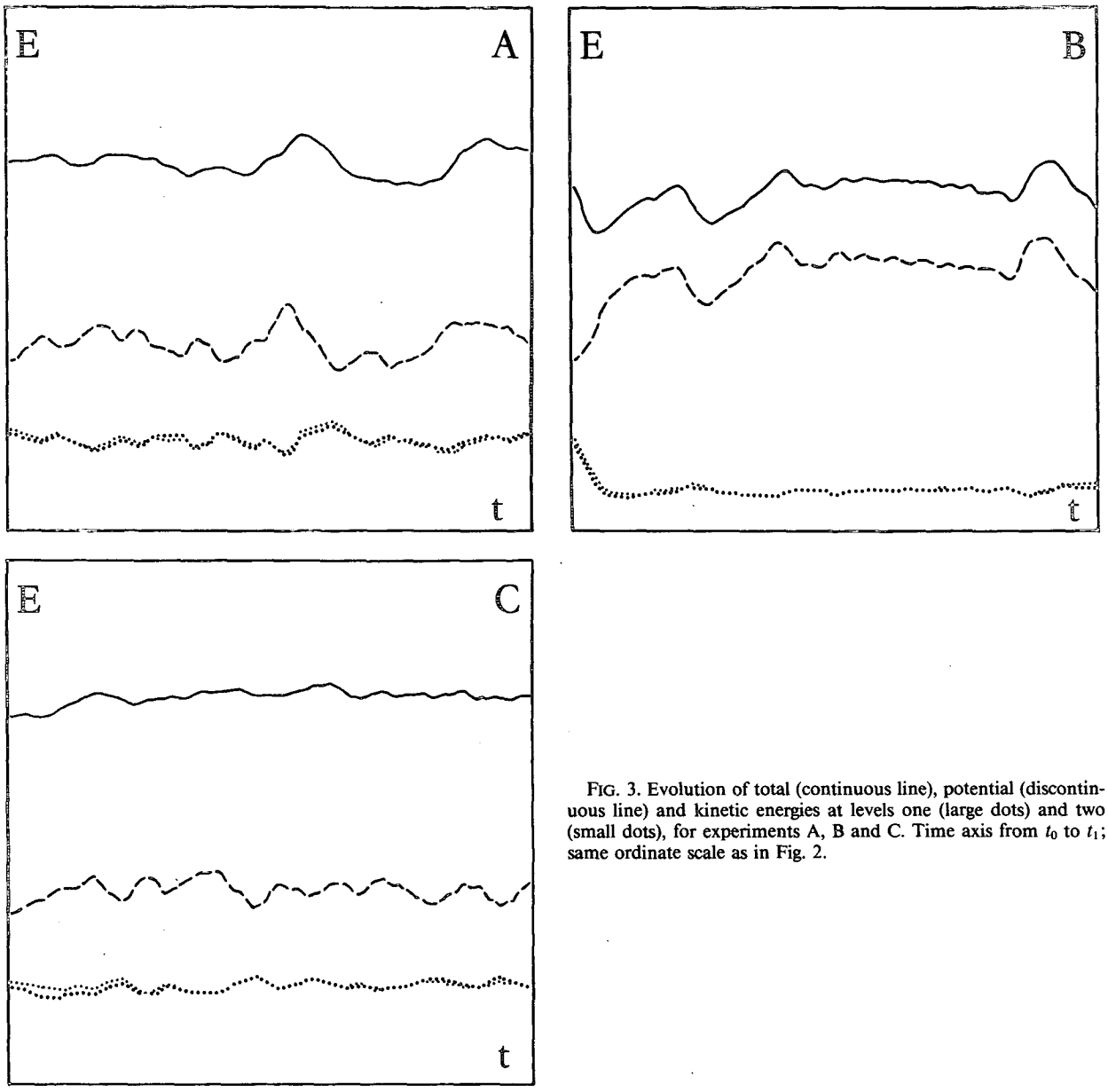

FIG. 3. Evolution of total (continuous line), potential (discontinuous line) and kinetic energies at levels one (large dots) and two (small dots), for experiments A, B and C. Time axis from t_0 to t_1; same ordinate scale as in Fig. 2.

with, again, $\beta = 8$, and $\tau \sim Z^{-1/2}$. Here we have no stability problem since the diffusion operator is linear; the resulting exponential decay term can be calculated exactly.

4. Numerical experiments

The numerical experiments are performed with an internal deformation wavenumber $\lambda = 15$. We first integrate a high resolution version of the model (128 $\times$ 128 points, $k_c = 61$), using the iterated Laplacian (16) for P^l, and pursue the integration long enough to reach a stationary flow regime. In this stationary regime we choose an initial time t_0; the high resolution simulation starting at $t = t_0$ and ending at $t = t_1$, with $t_1 = t_0 + 18000\Delta t$, will be referred to as our control experiment, or experiment C.[2] We then perform two parallel experiments with a low resolution ($k_c = \lambda = 15$) version of the model, using either the iterated Laplacian (experiment B), or the APVM (experiment A).

The choice $k_c = \lambda$ corresponds to a rather severe truncation for baroclinic eddies. It has been shown (Hoyer and Sadourny, 1982) that, in fully developed

[2] In physical units, the length of our simulation is $t_1 - t_0 = 1150 \times (\lambda U)^{-1}$, where U is the rms. velocity, or $t_1 - t_0 = 1620Z^{-1/2}$.

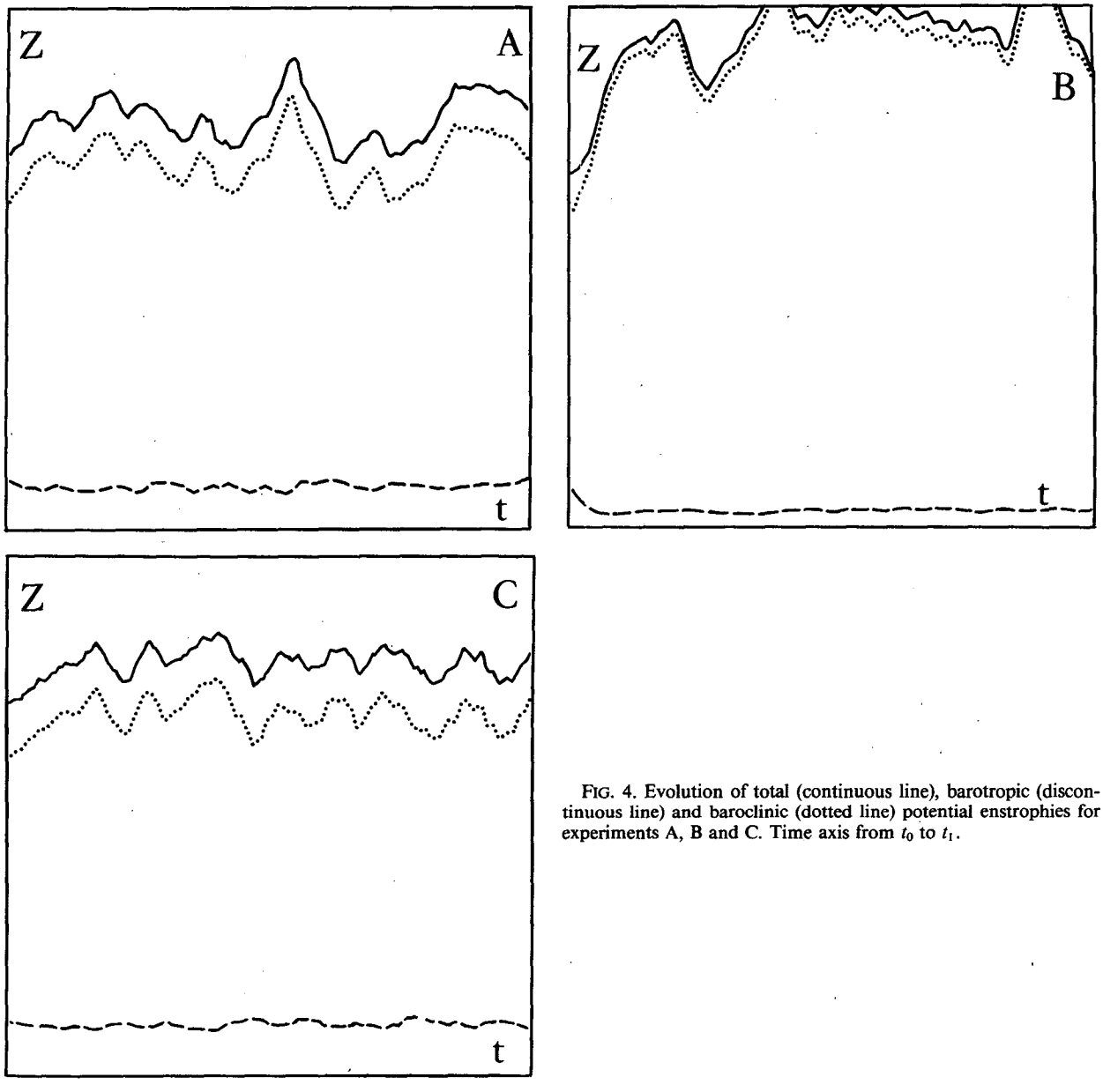

FIG. 4. Evolution of total (continuous line), barotropic (discontinuous line) and baroclinic (dotted line) potential enstrophies for experiments A, B and C. Time axis from t_0 to t_1.

quasi-geostrophic turbulence, nearly one-half of the energy or potential enstrophy transfers associated with baroclinic instability take place at $k > \lambda$, in contrast to the linear theory of parallel flow instability which predicts a baroclinically unstable range restricted to $k < \lambda$. (The linear theory is rather misleading in this respect, because it does not take into account interactions between eddies.) For both experiments A and B the initial state is the high resolution flow at $t = t_0$, truncated at $k_c = 15$. The thermal forcing field (13) shown in Fig. 1, has been actually truncated at $k = 8$ to retain only large-scale features; we have therefore strictly identical forcings in all three experiments. Also, we have truncated all the output fields of our control experiment C at $k = \lambda = 15$, in order to make them strictly comparable to their A and B counterparts. Note that the low resolution models A and B are integrated using a larger time step: $\Delta t' = 4\Delta t$.

a. Integral quantities

Figure 2 shows the evolution of total, barotropic and baroclinic energies

$$E = \hat{E}^0 + \hat{E}^1,$$

$$\hat{E}^0 = -\int\int_\Omega \hat{\psi}^0 \hat{\eta}^0 dxdy,$$

$$\hat{E}^1 = -\int\int_\Omega \hat{\psi}^1 \hat{\eta}^1 dxdy.$$

Our first remark is that E remains approximately constant in all three experiments, with a tendency for low-resolution simulations to produce larger fluctuations around the mean. In the control case, we observe an approximate equipartition of energy into its barotropic and baroclinic components (with a slight advantage, however, to baroclinic energy). This behavior is well reproduced in experiment A; in experiment B, on the contrary, we observe a dramatic increase of baroclinic energy in the first two thousand steps, accompanied by an even more intense decrease of barotropic energy. This behavior, in agreement with the EDQNM closure model simulations of Sadourny and Hoyer (1982), clearly shows the inability of classical lateral diffusion schemes to maintain the proper potential-to-kinetic energy conversion rate. The evolution of potential energy

$$P = \lambda^2 \int\int_\Omega (\hat{\psi}^1)^2 dxdy$$

and kinetic energy at $l = 1, 2$

$$K^l = -\frac{1}{2} \int\int_\Omega \psi^l \nabla^2 \psi^l dxdy$$

are also shown on Fig. 3. We verify that

$$P = \hat{E}^1, \quad K \equiv K^1 + K^2 = \hat{E}^0$$

is a good approximation; further, we have, approximately,

$$K^1 = K^2,$$

an assumption widely used in closure modeling (e.g., Salmon, 1980; Hoyer and Sadourny, 1982).

Figure 4 displays the evolution of total, barotropic and baroclinic potential enstrophies

$$Z = \hat{Z}^0 + \hat{Z}^1,$$

$$\hat{Z}^0 = \int\int_\Omega (\hat{\eta}^0)^2 dxdy,$$

$$\hat{Z}^1 = \int\int_\Omega (\hat{\eta}^1)^2 dxdy.$$

We note that $\hat{Z}^1$ evolves in a manner very similar to $\hat{E}^1$ (in fact, $\hat{Z}^1 \approx \lambda^2 \hat{E}^1$). Comparing experiment B to the control case, we again notice a clear degradation of potential enstrophy partition into its barotropic and baroclinic components. Experiment B is also unable to maintain the proper amount of total energy and potential enstrophy. Here we observe a slight decrease of E, and a more pronounced increase of Z: increasing τ would tend to counteract the energy decrease, but this would be at the expense of stronger enstrophy increase—and vice versa. In experiment A, Z, $\hat{Z}^0$ and $\hat{Z}^1$ are well maintained around their control values, although we observe again a tendency to produce larger fluctuations around the mean.

b. Energy spectra

A more detailed insight on the behavior of the diffusion operators is to be found in time-average energy spectra in the wavenumber band $(1, \lambda)$ (Fig. 5). The control baroclinic and barotropic energy spectra are quite well reproduced by experiment A, even in the close vicinity of the cutoff wavenumber; this means that the potential-to-kinetic energy conversions are statistically well captured by the APVM. On the other hand, experiment B overestimates baroclinic energy in the medium wavenumber range and underestimates barotropic energy in large wavenumbers; a portion of thermal energy thus remains in baroclinic form and is not available for the reverse energy cascades which feeds the barotropic large scales. In experiment B, we also observe strong dissipation ranges near the cutoff wavenumber in both barotropic and baroclinic spectra; another part of thermal energy is thus artificially dissipated and again is not available for the reverse energy cascade.

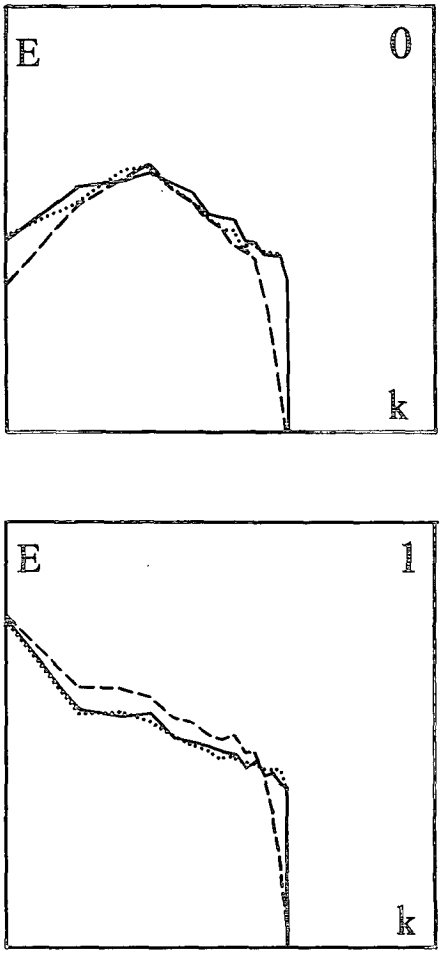

FIG. 5. Barotropic (0) and baroclinic (1) energy spectra for experiments A (APVM, dotted line), B (ordinary diffusion, discontinuous line) and C (high-resolution control, continuous line).

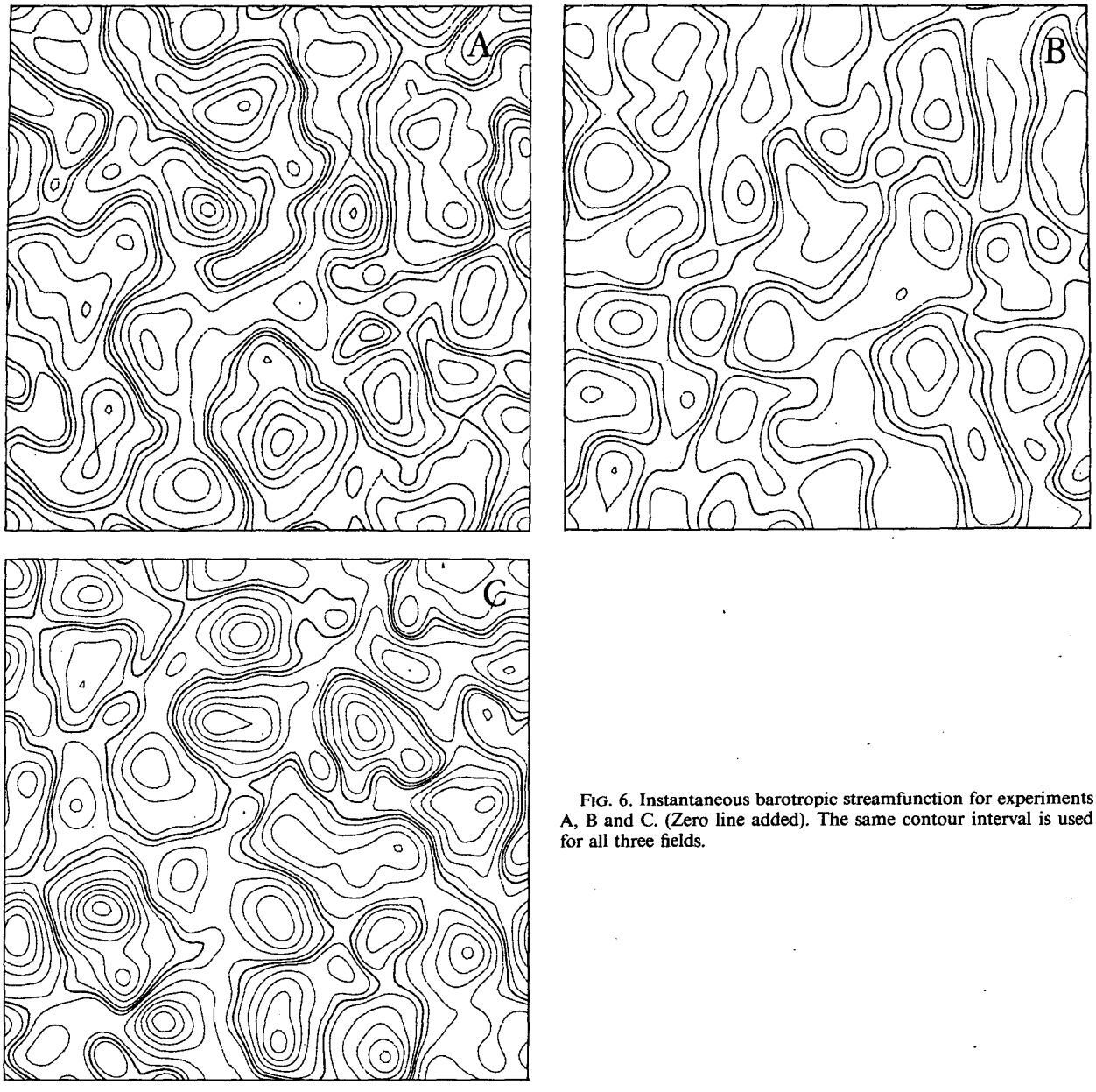

FIG. 6. Instantaneous barotropic streamfunction for experiments A, B and C. (Zero line added). The same contour interval is used for all three fields.

c. Streamfunctions

Figure 6 shows instantaneous barotropic streamfunction fields at $t_0 + 3000\Delta t$. Note that a simplified model like our quasi-geostrophic model on the periodic plane cannot simulate realistic large-scale barotropic structures, since there is no natural way to force mean zonal momentum. For this reason we expect the time-average barotropic streamfunction to vanish. Also, we are far beyond predictability limits; this means that we must not expect to recognize, in experiments A or B, any individual feature of the control experiment, and the similarity of the fields must be evaluated from a statistical standpoint in terms of resemblance of scale and amplitude distributions. The general weakening of barotropic flow structures in experiment B is conspicuous; experiment A, on the contrary, agrees quite well with the control sample.

The baroclinic streamfunctions (or temperatures), displayed on Fig. 7, have been time-averaged over 174 samples $96\Delta t$ apart from one another. Again we observe a fair agreement of experiment A with the control, while experiment B leads to a marked overestimation of mean temperature gradients, consistent with the weakening of baroclinic instability mecha-

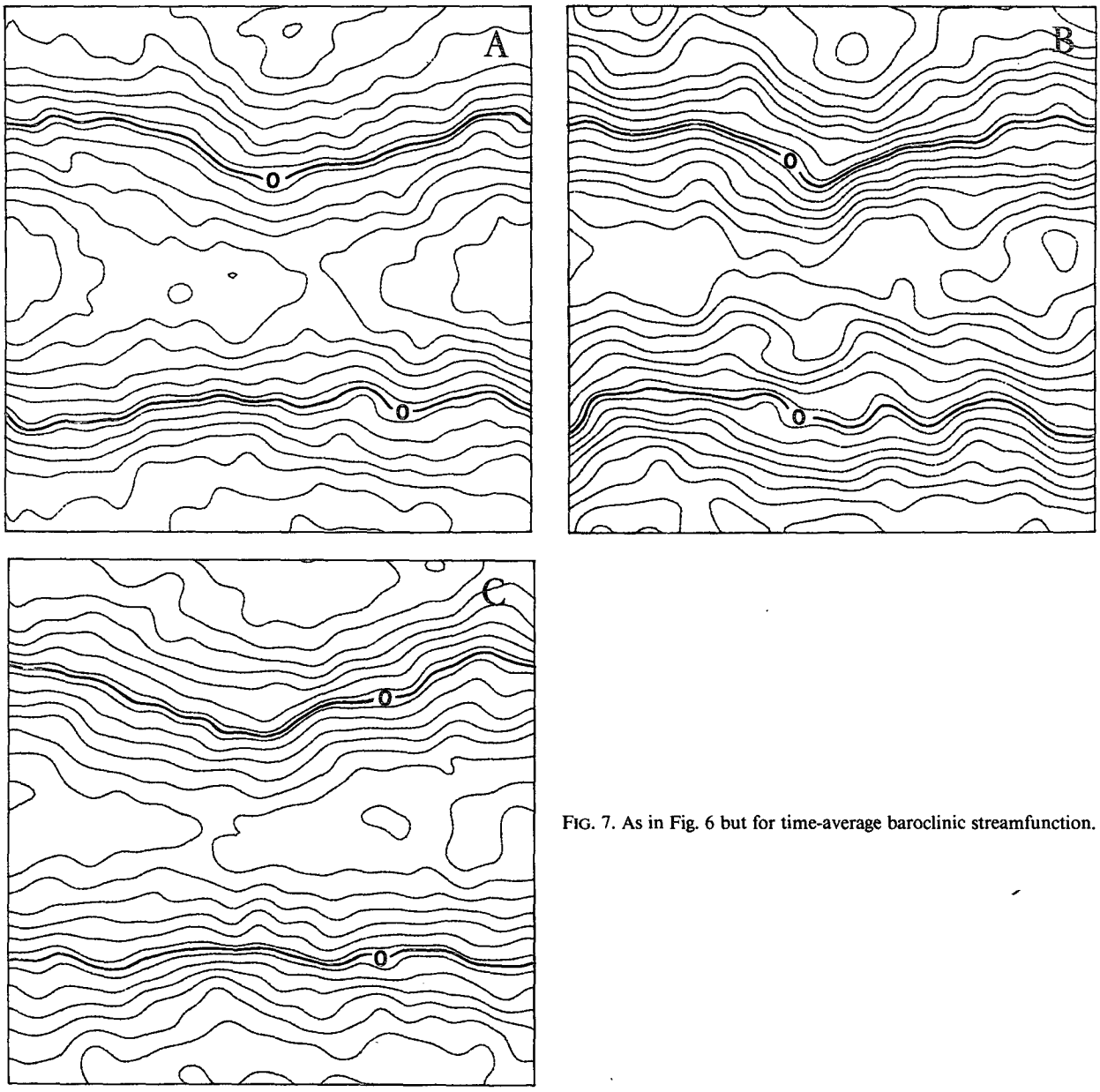

FIG. 7. As in Fig. 6 but for time-average baroclinic streamfunction.

nisms in that case. The agreement between A and C indeed shows that the APVM is able to reconstruct the correct magnitude of heat and potential vorticity fluxes, which are usually underestimated in coarse resolution models.

d. General comments

The problem we have considered here is the problem of parameterizing the subgrid scale heat and momentum fluxes in a baroclinic quasi-geostrophic model. Our results are therefore difficult to compare with previous works on estimating the meridional eddy heat fluxes from a prescribed zonally average temperature profile (e.g., Stone, 1974). Here what is prescribed is not the temperature profile but rather the rate of energy input (roughly in available potential form). Then, the long-term average meridional eddy heat fluxes which must equilibrate the energy source in any stationary regime phase are also practically prescribed. In such conditions, the effect of resolution and subgrid scale parameterization on the model's response is mainly seen by looking at the amplitudes of the mean meridional temperature profile obtained in each case. These are displayed on Table 1 for our three experiments A, B, C. We verify again that

TABLE 1. Amplitude of the zonally average meridional temperature profile (in arbitrary units) for the three experiments A, B, C.

	Experiment		
	A	B	C
$\Delta\bar{\psi}^1$	11.7	15.0	12.5

lowering the resolution with an ordinary diffusion scheme (going from C to B) yields an unrealistic enhancement of the mean meridional temperature gradient. This artificial enhancement totally vanishes with the APVM, which appears even more efficient at transporting heat than our control case; this is indeed encouraging, because we cannot expect our control case, with its modérate resolution and ordinary diffusion, to be as efficient as the exact equations.

5. Conclusion

The APVM is a lateral diffusion scheme constructed to obey the two generic properties of fully developed quasi-geostrophic turbulence: energy conservation and potential enstrophy dissipation. The technique is applicable to the quasi-geostrophic vorticity equation, or to the primitive equations using entropy as vertical coordinate. Its ability to model the subgrid scale barotropic–baroclinic instability processes is demonstrated here on a coarse-resolution, two-layer quasi-geostrophic model: the APVM succeeds in generating the expected vigorous large-scale barotropic structures, which standard lateral diffusion schemes are unable to do in a realistic way.

The reason why the APVM succeeds in parameterizing the subgrid scale barotropic–baroclinic instability processes is easy to explain. Being potential enstrophy dissipating, it has to produce the right amount of potential enstrophy dissipation in stationary regime conditions (simulating a transfer of potential enstrophy to subgrid scales roughly equal to potential enstrophy injection). Being, in addition, energy conserving, the APVM forces this potential enstrophy transfer to be reflected in the energetics as a correct amount of potential to kinetic energy conversion, without any dissipative loss. The parameters in the AVPM are a set of wavenumber-dependent time scales θ_k, whose spectral distribution should not affect the gross properties stated above, but of course influence the resulting spectral repartitions of barotropic and baroclinic energy; a highly scale-selective distribution (here $\sim k^{16}$) seems to yield quite realistic spectra.

The present tests have been performed in the case of two-layer "internal" baroclinic flow within isentropic upper and lower boundaries. This is one of the simplest cases, but we may expect similar performance for the "external" two-vertical mode problem (uniform potential vorticity flow with upper and lower boundary frontogenesis: Blumen, 1978) which reduces to the same formalism if one replaces potential enstrophy by available potential energy on boundaries (Hoyer and Sadourny, 1982); and for the multilayer internal problem. A discussion of the fully developed "external" and multilayer "internal" baroclinic instability problems and their implications for subgrid scale parameterization is given in Sadourny (1985); it shows that the basic properties of the APVM in terms of being able to simulate the energy cycle in coarse resolution models are readily extended to these cases. Of course, including higher order vertical modes in a model with given horizontal resolution means more severe truncation effects for the shallower instability modes (smaller deformation radii); this, however, should not affect too much the APVM efficiency, which mainly requires the energy sources to be resolved.

The ultimate goal here is, of course, the development of a parameterization scheme for the primitive equations, which may then be utilized in climate studies or general circulation studies. Regarding this goal, we may expect that a method which works well in the quasi-geostrophic case should work reasonably well for the primitive equations. The only problem, as we have shown, is that a straightforward formulation of the APVM in the primitive equation case requires the use of entropy as vertical coordinate. Entropy-coordinate short range forecasting models are indeed available (e.g., Eliassen and Raustein, 1967; Bleck, 1974), but entropy-coordinate general circulation models, robust enough for long-term simulations, have yet to be developed.

REFERENCES

Babiano, A., C. Basdevant and R. Sadourny, 1984: Le spectre d'énergie d'un écoulement turbulent bi-dimensionnel est-il mesurable? *C.R. Acad. Sci. Paris,* **299,** 495–498.

——, ——, B. Legras and R. Sadourny, 1984: Dynamiques comparées du tourbillon et d'un scalaire passif en turbulence bidimensionnelle incompressible. *C.R. Acad. Sci. Paris,* **299,** 601–604.

Basdevant, C., and R. Sadourny, 1983: Modélisation des échelles virtuelles dans la simulation numérique des écoulements turbulents bidimensionnels. *J. Méc. Pure Appl. No Spécial on Two-Dimensional Turbulence,* 243–269.

——, M. Lesieur and R. Sadourny, 1978: Parameterization of subgrid scale enstrophy transfer in two-dimensional turbulence. *J. Atmos. Sci.* **35,** 1028–1042.

——, B. Legras, R. Sadourny and M. Béland, 1981: A study of barotropic flows: Intermittency, waves and predictability. *J. Atmos. Sci.,* **38,** 2305–2326.

Bleck, R., 1974: Short-range prediction in isentropic coordinates with filtered and unfiltered models. *Mon. Wea. Rev.,* **102,** 813–829.

Blumen, W., 1978: Uniform potential vorticity flow. Part 1: Theory of wave interactions and two-dimensional turbulence. *J. Atmos. Sci.,* **35,** 774–783.

Eliassen, A., and E. Raustein, 1967: A numerical integration

experiment with a model atmosphere based on isentropic surfaces. *Ann. Meteor.*, **5,** 45–63.

Green, J. S. A., 1970: Transfer properties of the large-scale eddies and the general circulation of the atmosphere. *Quart. J. Roy. Meteor. Soc.*, **96,** 157–185.

Held, I. M., 1978: The vertical scale of an unstable baroclinic wave and its importance for eddy heat flux parameterizations. *J. Atmos. Sci.*, **35,** 572–576.

Hoyer, J. M., and R. Sadourny, 1982: Closure modeling of fully-developed baroclinic instability. *J. Atmos. Sci.*, **39,** 707–721.

Kraichnan, R. H., 1976: Eddy viscosity in two and three dimensions. *J. Atmos. Sci.*, **33,** 1521–1536.

Leith, C. E., 1968: Diffusion approximation for two-dimensional turbulence *Phys. Fluids,* **11,** 671–673.

McWilliams, 1984: The emergence of isolated coherent vortices in turbulent flow. *J. Fluid Mech.*, **146,** 21–43.

Sadourny, R., 1985: Techniques for numerical simulation of large-scale eddies in geophysical fluid dynamics. *Large Scale Computations in Fluid Mechanics, Lectures in Applied Math.*, 22, (in press).

——, and C. Basdevant, 1981: Une classe d'opérateurs adaptés à la modélisation de la diffusion turbulente en dimension deux. *C.R. Acad. Sci. Paris,* **292,** 1061–1064.

——, and J. M. Hoyer, 1982: Inhibition of baroclinic instability in low-resolution models. *J. Atmos. Sci.*, **39,** 2138–2143.

Saltzman, B., 1968: Steady-state solutions for the axially-symmetric climatic variables. *Pure Appl. Geophys.*, **69,** 237–259.

Stone, P. H., 1974: The meridional variation of the eddy heat fluxes by baroclinic waves and their parameterization. *J. Atmos. Sci.*, **31,** 444–456.

——, 1978: Baroclinic adjustment. *J. Atmos. Sci.*, **35,** 561–571.